VIRTUAL SCREENING OF CYANOBACTERIAL METABOLITES AS INHIBITORS OF SARS-CoV-2 HOST CELL ENTRY, VIRAL REPLICATION, AND HOST IMMUNITY MODULATION INFECTIVE MECHANISMS

Viktor Aloysius A. Fellizar[1,2], Aaron Cyrus A. Concepcion[1,2], Emmanuel Louise A. Furaque[1,2], Angela Maxine G. Fabian[1,2], Von Novi O. de Leon[1,3], Delfin Yñigo H. Pilapil IV[1,3], Mark Tristan J. Quimque[1,5,6], Kin Israel R. Notarte[1,4], Allan Patrick G. Macabeo[1*]

[1]Laboratory for Organic Reactivity, Discovery, and Synthesis (LORDS), Research Center for the Natural and Applied Sciences, University of Santo Tomas, España Blvd., Manila 1015 Philippines

[2]Science, Technology, Engineering, and Mathematics (STEM), Senior High School, University of Santo Tomas, España Blvd., Manila 1015 Philippines

[3]Department of Biological Sciences, College of Science, University of Santo Tomas, España Blvd., Manila 1015 Philippines

[4]Faculty of Medicine and Surgery, University of Santo Tomas, España Blvd., Manila 1015 Philippines

[5]Department of Chemistry, College of Science and Mathematics
Mindanao State University-Iligan Institute of Technology
Tibanga, Iligan City 9200 Philippines

[6]The Graduate School, University of Santo Tomas
España Blvd., Manila 1015 Philippines

Correspondence: agmacabeo@ust.edu.ph

ABSTRACT

The novel severe acute respiratory syndrome coronavirus (SARS-CoV-2) emerged in December 2019 leading to a global pandemic and lockdowns in different countries including the Philippines. There is an oral antiviral treatment, Paxlovid, produced by Pfizer that is currently authorized for emergency use to treat COVID-19. However, there is still a necessity to discover specific antiviral drugs due to increasing cases worldwide. In this study, 56 cyanobacterial secondary metabolites were virtually screened for *in silico* inhibitory prospects against five main targeted proteins of SARS-CoV-2 involved in viral attachment, viral replication, and host immunity modulation mechanisms. Pharmacokinetic properties and toxicity predictions were also performed. Of the fifty-six secondary metabolites molecularly docked, compounds **1**–**7** showed favorable binding energy ranging from -

10.9 to -8.0 kcal/mol against the spike's ACE2 (angiotensin-converting enzyme 2) and GRP 78 (glucose-related protein 78) receptor binding domains, $3CL^{PRO}$ (3-chymotrypsin-like protease), PL^{PRO} (papain-like protease), and RdRp (RNA-dependent RNA-polymerase). Three compounds, scytonemin (**1**) a bisindole alkaloid dimer, cryptophycin (**5**) a macrolactam, and tjipanazole A2 (**6**) an indole alkaloid glucoside exhibited highest the binding affinities with BE's ranging from -10.4 to -8.6 kcal/mol. Top-ranked ligands **1**–**7** also demonstrated favorable pharmacokinetics with low toxicity risks.

Keywords: COVID-19, SARS-CoV-2, cyanobacterial metabolites, molecular docking, antiviral, ADMET

INTRODUCTION

The emergence of the novel coronavirus, SARS-CoV-2, poses a global health threat causing the COVID-19 pandemic, which first exhibited a series of infections as viral pneumonia in Wuhan, China and as of 12 January 2022, the World Health Organization tallied a record of 312 million COVID-19 cases with 5.50 million deaths (Harapan et al., 2020). SARS-CoV-2 is a positive-sense, single-stranded RNA virus that belongs to the genus Betacoronavirus, which commonly infects bats, humans, and other mammals (Aftab et al., 2020). Viral transmission is complex and governed by a range of factors including host cell entry and occurs a host-mediated inhibition that determines the likelihood of successful infection; thus, host cell entry and host immunity modulation present as treatment targets. Viral spread is through contact with respiratory beads from cough and sneeze of a contaminated individual. With the ease of spread and limited treatment options, it is alarming for people in fighting COVID-19 (Albano, 2020; Conceicao et al., 2020). To this date, the oral anti-COVID-19 drug Paxlovid produced by Pfizer is authorized for emergency use for treating the disease. According to Pfizer, this drug was designed to target the SARS-CoV-2 $3CL^{PRO}$ utilizing the compound PF-07,321,322 that binds to the catalytic cysteine residue, Cys145, found in most coronavirus proteases that infect humans (Drożdżal et al.,2021).

In this study, $3CL^{PRO}$ is also a target protein, and considering the continuous mutation of SARS-CoV-2 and the presence of different variants, the target protein for the drug and in this study is highly conserved. In addition, $3CL^{PRO}$ is an nsp, that are enzymes that have important roles in viral replication and life cycle of the virus that might modulate host responses to infection (Khateeb et al., 2021; van Dorp et al., 2020).

The use of computer-aided drug design and discovery (CADDD) has accelerated drug development to streamline efforts and time in the discovery of compounds for *in vitro* and *in vivo* experimental studies (Chaudhary & Mishra, 2016). Among the numerous applications of CADDD is the use of molecular docking, which is commonly used in the discovery for treatment against SARS-CoV-2 (de Leon et al., 2021; Fernandez et al., 2021). This strategy is a promising method since it plays a major role in efforts for modern drug discovery and development particularly anti-COVID-19 drugs (Brogi et al., 2022). With this, virtual screening is a promising method in streamlining compounds to find novel drug leads from secondary metabolites to enrich their biological and pharmacokinetic activities that could potentially be treatments against SARS-CoV-2 (Brogi et al., 2022; Chaudhary & Mishra, 2016; M. T. Quimque et al., 2021).

Cyanobacterial secondary metabolites showcase a wide range of potential biological activities such as antiviral, anticancer, antibacterial, antifungal, antialgal, antimalarial, antimycotic, and antitumor properties (Raja et al., 2016; Rastogi & Sinha, 2009). Despite the established range of biologically active cyanobacterial metabolites against certain target diseases, studies related to their anti-viral activity are limited. Thus, fifty-six secondary metabolites from marine and terrestrial cyanobacteria were screened *in silico* as antagonists to the spike receptor-binding domains (RBD) to angiotensin-converting enzyme 2 (ACE2) and glucose-related protein 78 (GRP 78), which are essential for host cell recognition and entry; 3-chymotrypsin-like protease ($3CL^{PRO}$) and RNA-dependent RNA-polymerase (RdRp) for viral replication; and papain-like protease (PL^{PRO}), implicated in host immunity modulation. In this paper, we present top seven cyanobacterial metabolites that showed multi-targeting *in silico* antagonisms to SARS-CoV-2

target proteins, along with the computational predictions for pharmacokinetic properties and toxicity risks.

MATERIALS AND METHODS

Target Enzyme/Structural Protein Preparation

Two target protein sites important for infectivity, spike RBDs for ACE2 and GRP78; and three non-structural proteins of SARS-CoV-2, RdRp, $3CL^{PRO}$, and PL^{PRO}, were chosen as molecular targets. The three-dimensional crystal structures of the following target proteins were retrieved from the RCSB protein data bank (RCSB.org): spike's receptor-binding domain (RBD) to GRP78 (PDB ID: 6VXX) and ACE2 receptors (PDB ID: 6M0J), RdRp (PDB ID: 6M71), 3CLPro (PDB ID: 6LU7), and PLPro (PDB ID: 6W9C) (Fernandez et al., 2021; Quimque et al., 2021). Three-dimensional structures of the enzymes in the PDB format were rendered in the UCSF Chimera platform (Pettersen et al., 2004) (Figure 1).

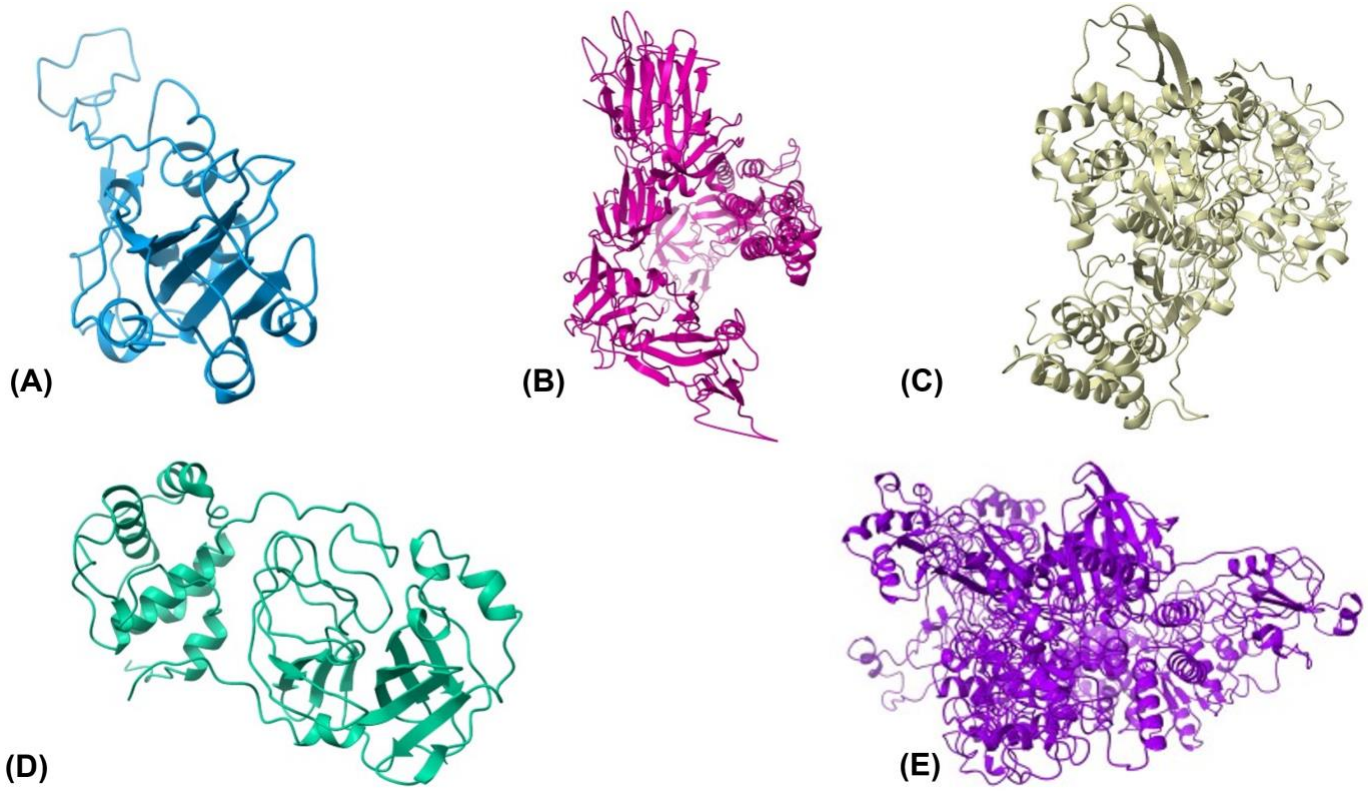

Figure 1. 3-Dimensional Structures of SARS-CoV-2 [A] spike RBD for ACE2, [B] spike RBD for GRP78, [C] RdRp, [D] $3CL^{PRO}$, and [E] PL^{PRO}.

Ligand Selection and Preparation

A library of fifty-six (56) metabolites from cyanobacteria with no known antiviral properties from previous works were screened *in* silico against SARS-CoV-2 target proteins. The ligands were rendered as SYBYL mol2 files in an open-source molecular build software, Avogadro (version 1.1.1) (Hanwell et al., 2012). These ligands were added to the UCSF Chimera platform for molecular docking.

Molecular Docking Simulations

Molecular docking experiments were conducted on the UCSF Chimera platform (Pettersen et al., 2004). The three-dimensional structures of the protein were added to the docking platform as PDB formats. Each protein crystal structure was detached prepared by removing existing co-crystallized ligands and water molecules. On the other hand, the SYBYL mol2 file

ligands were added to the docking platform. The minimization and docking preparation of both the ligand and protein structures was done by supplying the missing hydrogen atoms and assigning charges *via* Gasteiger method, calculated using Amber's Antechamber module (Wang et al., 2006).–The docking procedure was done by using a "flexible ligand into a flexible active site" protocol (Africa et al., 2022). With all docking parameters set at default values, the molecular docking simulation was performed following the Broyden-Fletcher-Goldfarb-Shanno (BFGS) algorithm of AutoDock Vina (version 1.1.2) (Quimque et al., 2021). After each run, Autodock Vina supplied a set of docking poses for each ligand with calculated binding affinities. The docking model with best affinity was chosen to represent the set and was subjected to post-dock analysis. Visualization and analysis of the enzyme-ligand interactions and residues were done through UCSF Chimera and BIOVIA Discovery Studios (version 4.1) (Africa et al., 2022; de Leon et al., 2021; Fernandez et al., 2021).

Drug-likeness, ADME, and Toxicity Prediction

Drug-likeness of the compounds were determined according to Lipinski's 'rule-of-five' which examines the biochemical features of a drug that may affect its absorption and permeation across cell membranes. The computational prediction of the absorption, distribution, metabolism, and excretion (ADME) properties of compounds **1**–**7** which showed *in silico* antagonism was observed using SwissADME (Daina et al., 2017; Quimque et al., 2021). Moreover, OSIRIS Property Explorer program was employed for *in silico* toxicity prediction which includes the potential mutagenicity, tumorigenicity, irritant effects, and reproductive toxicity of the hit compounds (Phukhamsakda et al., 2019). Having the same software, the solubility (Log *S*) of hits which is a cause for absorption and bioavailability was also forecasted. Values of Log S equal or greater than -4 are expressive of favorable solubility (Escobedo-Gonzales et al., 2017).

RESULTS

Molecular Docking Analysis

A library of fifty-six cyanobacterial metabolites was screened *in silico* to SARS-CoV-2 spike RBD to ACE2 and GRP78, RdRp, $3CL^{PRO}$, and PL^{PRO} involved in host cell entry, host immunity modulation, and viral replication. Compounds **1**, **3**, **5**, **7**, and **2** manifested as the top-ranking ligands with high binding affinities to each of the target proteins (Figure 2; Table 1). The top compounds **1**–**7** were further assessed for drug-likeness and toxicity *in silico*.

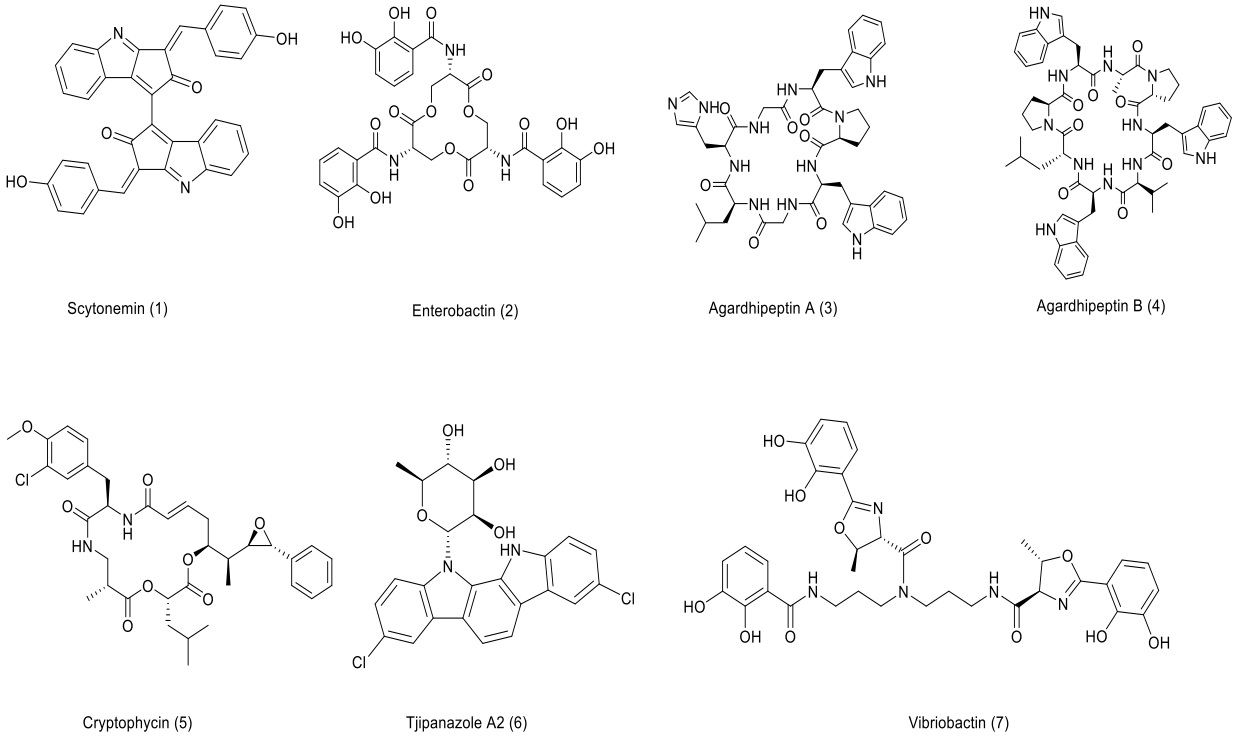

Figure 2. Cyanobacterial metabolites **1-7** with high binding affinities against SARS-CoV-2 spike receptor-binding domains for ACE2 and GRP78; and nonstructural proteins, RdRp, $3CL^{PRO}$, and PL^{PRO}.

Table 1. Binding energies of cyanobacterial metabolites (**1-7**) expressed in kcal/mol to SARS-CoV-2 target proteins.

Target	Compound	Binding Affinity (kcal/mol)
ACE2	**1**	-8.6
	3	-8.6
	2	-8.1
GRP78	**3**	-8.6
	4	-8.3
	1	-8.2
RdRp	**1**	-9.3
	5	-9.2
	6	-8.6
$3CL^{PRO}$	**1**	-8.8
	7	-8.4
	2	-8.0
PL^{PRO}	**3**	-10.9
	2	-10.9
	1	-10.4

Molecular Docking with Spike RBD for ACE2

Scytonemin (**1**)**,** a lipopeptide isolated from *Scytonema* sp. (Nowruzi et al., 2018; Rastogi & Sinha, 2009), exhibited a high binding affinity with a BE of -8.6 kcal/mol to spike RBD ACE2. Post-docking analysis showed a series of molecular interactions such as conventional hydrogen bonds with Ser162, Gln161, and Gln166 of the spike ACE2 RBD, a *pi-pi*-stacked interaction with Tyr173, and a *pi*-donor hydrogen attraction with Gly170 (Table 2).

Agardhipeptin (**3**)**,** a cyanobacterial peptide isolated from *Oscillatora agardhii* (Shin, H. J., Matsuda, H., Murakami, M., & Yamaguchi, K. 1996) also exhibited a high binding affinity of -8.6 kcal/mol to spike RBD ACE2. Post-docking analysis of molecular interactions revealed conventional hydrogen bonds with Gly164, Ser162, and Tyr121 of the spike ACE2 RBD, a carbon-hydrogen bond with Tyr163, and a *pi-pi* stacked interaction with Tyr117.

Lastly, enterobactin (**2**), a non-ribosomal peptide isolated from enterococci (Gademann & Portmann, 2008) exhibited a binding affinity of -8.1 kcal/mol to spike RBD ACE2. Post-docking analysis showed conventional hydrogen bonds with Ser162, Gln161, Tyr117, Tyr121, and Arg71, and a *pi-sigma* interaction with Leu120.

Table 2. Summary of docking interactions with spike RBD ACE2

Ligand	Ligand/receptor docking interaction	Binding Affinity (kcal/mol)	Interactions
1	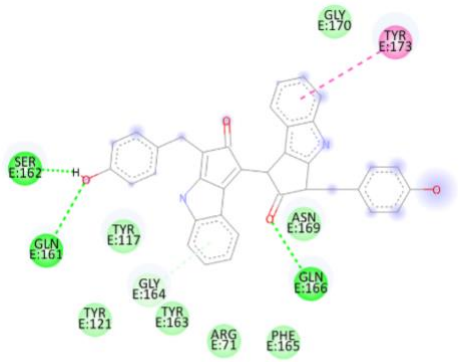	-8.6	Hydrogen Bonding with Ser162 and Gln161; π-π interactions with Tyr173.
3	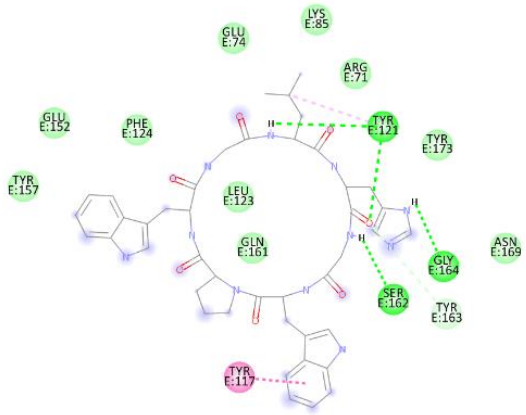	-8.6	Hydrogen Bonding with Tyr121, Gly164, and Ser162; π-Alkyl interactions with Tyr117 and Tyr121.

2	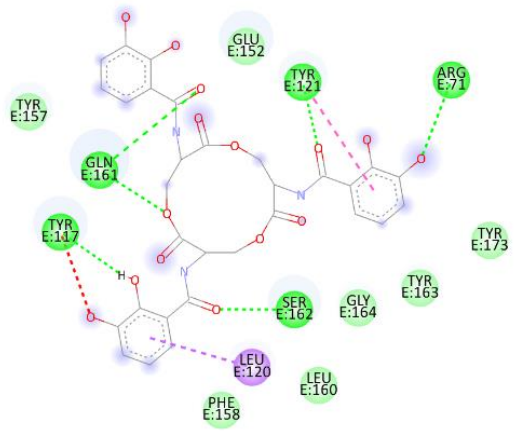	-8.1	Hydrogen Bonding with Gln161, Tyr117, Tyr121, Arg71 and Ser162; π-sigma interactions with Leu120.

Molecular Docking with Spike RBD for GRP-78

Aside from the spike RBD for ACE2, agardhipeptin A (**3**) exhibited a high binding affinity with a BE of -8.6 kcal/mol to spike GRP78 RBD. Post-docking analysis of molecular interactions revealed conventional hydrogen bonds with Ser373 and Gly380, carbon-hydrogen bond interactions with Asn385 and Gln382, a *pi-alkyl* interaction with Tyr388, and a *pi-cation* interaction with Lys300 (Table 3).

On the other hand, agardhipeptin B (**4**), a cyanobacterial peptide isolated from *Oscillatora agardhii* (Shin, H. J., Matsuda, H., Murakami, M., & Yamaguchi, K. 1996) exhibited a binding affinity of -8.3 kcal/mol to spike GRP78 RBD. Post-docking analysis showed a series of molecular interactions of a conventional hydrogen bond with Tyr364, a carbon-hydrogen bond with Tyr364,

pi-cation interactions with Lys330 and Arg316, *pi-pi* T-shaped interactions with Tyr379 and Tyr373, and a *pi-alkyl* bonding with Tyr360.

Scytonemin (**1**) exhibited a BE of -8.2 kcal/mol to spike GRP78 RBD. Post-docking analysis showed a series of molecular interactions of a conventional hydrogen bond with Leu376, an unfavorable acceptor-acceptor interaction with Ser378, a *pi-pi*-stacked interaction with Phe374, and a *pi-alkyl* interaction of Leu363.

Table 3. Summary of docking interactions with spike RBD GRP78

Ligand	Ligand/receptor docking interaction	Binding Affinity (kcal/mol)	Interactions
3	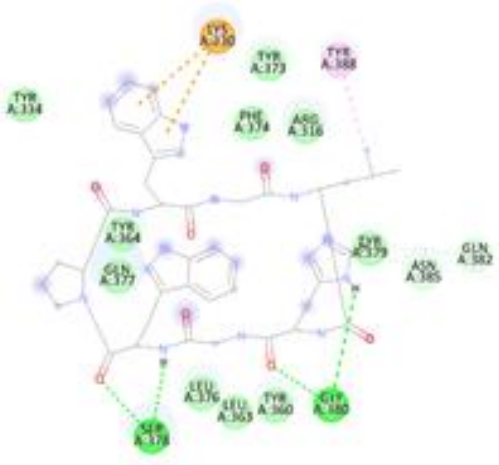	-8.6	Conventional Hydrogen Bond with Ser373 and Gly380; Carbon Hydrogen Bond with Asn385 and Gln382; π-Alkyl interaction with Tyr388; π-Cation interaction with Lys300 and Arg316; and π-π T-shaped interaction with Tyr379 and Tyr373.
4	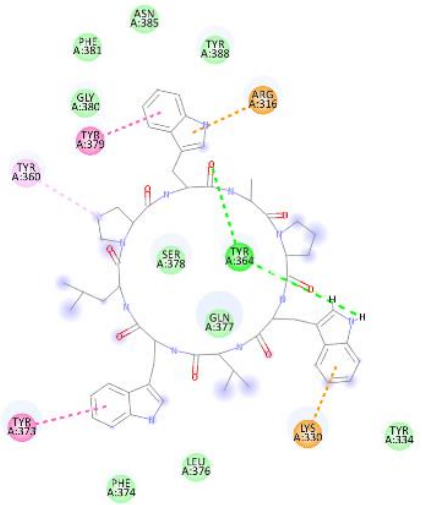	-8.3	Conventional Hydrogen bond of Tyr364; carbon hydrogen bond of Tyr364; π-Alkyl interactions with Tyr360; and π- Cation interaction with Lys330.

1	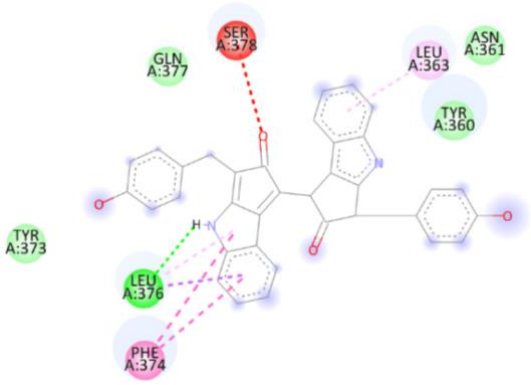	-8.2	Hydrogen Bonding with Leu376; π-π T-shaped interactions with Phe374; and π-Alkyl interactions Leu363.

Molecular Docking for 3CL^{PRO}

Scytonemin (**1**) exhibited a high binding affinity of -8.8 kcal/mol to 3CL^{PRO}. Post-docking analysis showed conventional hydrogen bonds with Arg188 and Gln189, a *pi*-donor hydrogen bond with His41, a *pi*-sulfur interaction with Cys145, *pi-pi* T-shaped interactions with Met49 and Met165, and *pi*-alkyl interaction with Leu50 and Leu27 (Table 4).

Vibriobactin (**7**) is an iron chelator isolated from cyanobacteria-*Vibrio cholerae* (Gademann & Portmann, 2008) exhibited a high binding affinity with a BE of -8.4 kcal/mol to 3CL^{PRO}. Post docking analysis revealed a series of conventional hydrogen bonds with Gln189, Glu166, Gly143, and Leu141, an unfavorable donor-donor interaction with Ser144, an alkyl interaction with Cys145, and *pi*-alkyl interactions with Met165, His164, and His41.

Enterobactin (**2**) exhibited a binding affinity of -8.0 kcal/mol to 3CL^{PRO}. Post docking analysis showed a series of conventional hydrogen bonds with Thr24, Gly143, Asn119, and

Gln19, an unfavorable donor-donor interaction with Gln19, a *pi*-donor hydrogen bond with His41, and a *pi-pi* stacked and *pi-pi* T-shaped interactions with Tyr118.

Table 4. Summary of docking interactions with $3CL^{PRO}$

Ligand	Ligand/receptor docking interaction	Binding Affinity (kcal/mol)	Interactions
1	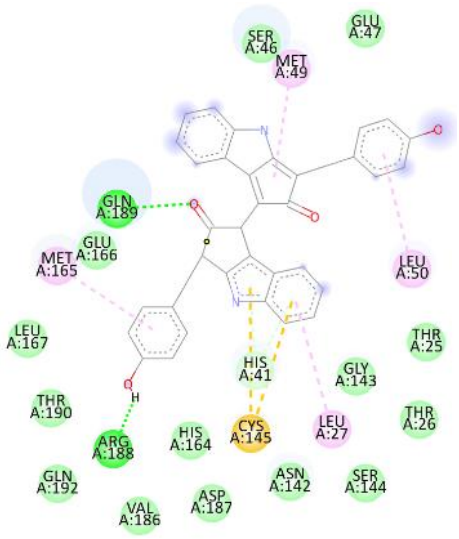	-8.8	Hydrogen Bonding with Gln189 and Arg188; π-Alkyl interactions with Met49, Leu50, Met165 and Leu2; π-Sulfur interactions with Cys145.
7	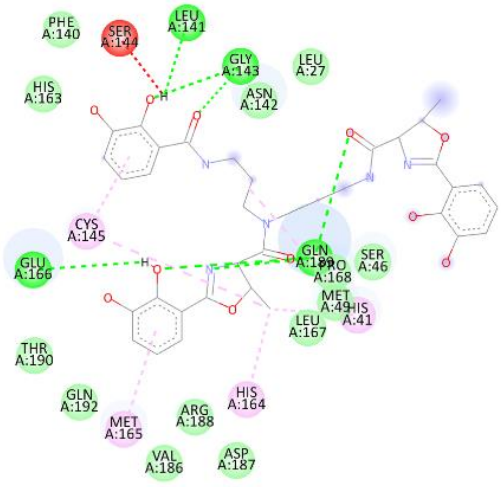	-8.4	Hydrogen Bonding with Ley141, Gly143, Gln189, and Glu166; π-Alkyl or alkyl interactions with Cys145, Met165, His164, and HIS41.

2	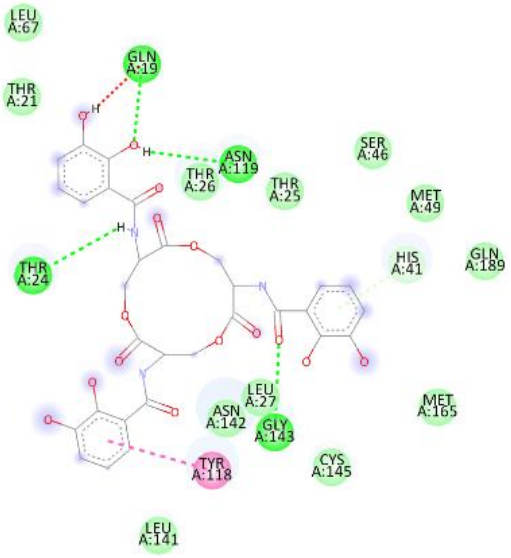	-8.0	Hydrogen Bonding with Gln19, Asn119, Thr24, and GLY143; and π-π Stacked interactions or π-π T-shaped interactions with Tyr118.

Molecular Docking with RNA-dependent RNA-polymerase (RdRp)

Scytonemin (**1**) exhibited a high binding affinity with a BE of -9.3 kcal/mol to RdRp. Post docking analysis of molecular interactions showed conventional hydrogen bonds with Lys740 and Tyr561, a carbon hydrogen bond interaction of Trp742, and *pi-pi*-stacked interactions of Arg495 and Asp702 (Table 5).

Cryptophycin (**5**), a depsipeptide cytotoxin isolated from a lipophilic extract of *Nostoc* sp. ATCC 53789 (Nowruzi et al., 2018; Rastogi & Sinha, 2009), exhibited a binding affinity of -9.2 kcal/mol to RdRp. Post docking analysis showed a series of conventional hydrogen bonds and

pi-alkyl interactions both with Lys563 and His752, *pi-alkyl* interactions with Trp742, Pro562, and Lys740, and *pi-anion* and *pi-cation* interactions with Glu753 and Lys740.

Tjipanazole A2 (**6**), an indole alkaloid isolated from *Tolypothrix tjipanasensis* (Gademann & Portmann, 2008), exhibited a binding affinity of -8.6 kcal/mol to RdRp. Post docking analysis showed a series of molecular interactions of conventional hydrogen bonds with Trp559 and Lys740, a carbon-hydrogen bond interaction with Trp559, and *pi-alkyl* interactions with Lys740 and His752.

Table 5. Summary of docking interactions with RdRp

Ligand	Ligand/receptor docking interaction	Binding Affinity (kcal/mol)	Interactions
1	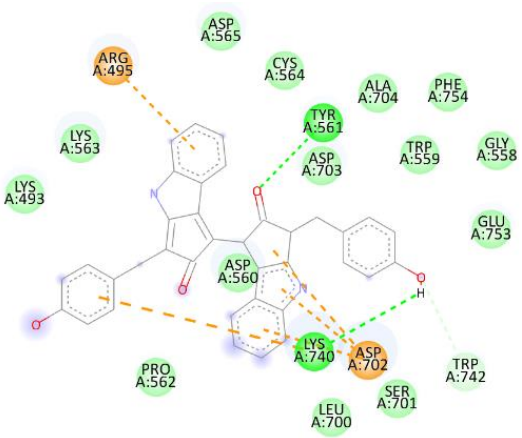	-9.3	Hydrogen Bonding with Tyr561 and Lys740; and π -Cation or π-Anion interactions with Arg495 and Asp702.
5	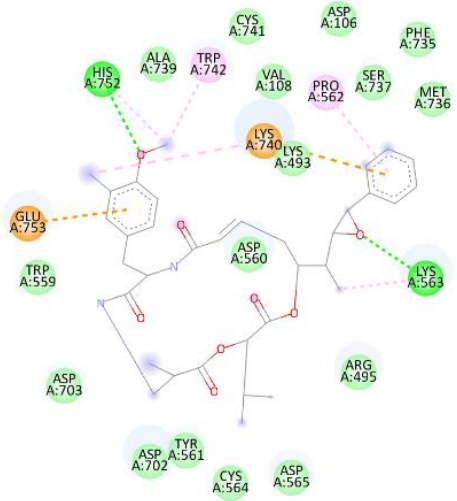	-9.2	Hydrogen Bonding with Lys563 and His752; π-Alkyl or alkyl interactions with Trp742 and Pro562; and π-Cation or π-Anion interactions with Lys740 and Glu753.

6	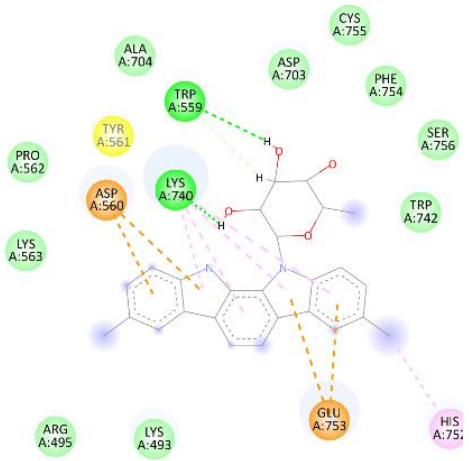	-8.6	Hydrogen Bonding with Trp559 and Lys740; π-alkyl interactions His752 and Lys740; π-sulfur interaction with Tyr561; and π-Anion interactions with Asp560 and Glu753.

Molecular Docking for PL^{PRO}

Agardhipeptin A (**3**) exhibited the highest binding affinity of -10.9 kcal/mol to PL^{PRO}. Post-docking analysis showed a series of conventional hydrogen bonds with Asp714, Asp309, Asp339, an unfavorable donor-donor interaction with Leu557, *pi*-cation and *pi*-anion interactions with Arg558 and Arg586, a *pi*-sigma interaction with Thr583, and *pi*-sigma interactions with Val635, Lys694, Arg712, and Ile310 (Table 6).

Enterobactin (**2**) exhibited a binding affinity with a BE of -10.9 kcal/mol to PL^{PRO}. Post-docking analysis showed a series of conventional hydrogen bonds with Thr583, Asp339, Arg558, Asp714, Lys711, and Val659, a *pi*-anion interaction with Asp339, and a *pi*-sigma interaction with Ile310.

Scytonemin (**1**) exhibited a binding affinity with a BE of -10.4 kcal/mol to PL^{PRO}. Post-docking analysis showed a series of conventional hydrogen bonds with Asp309, a *pi*-cation

interaction with Asp309, a *pi*-anion interaction of Lys751, a *pi*-sigma interaction with Val732, a *pi-pi* stacked interaction with Phe726, and a *pi*-alkyl interaction with Arg748.

Table 6. Summary of docking interactions with PL^{PRO}

Ligand	Ligand/receptor docking interaction	Binding Affinity (kcal/mol)	Interpretations
3	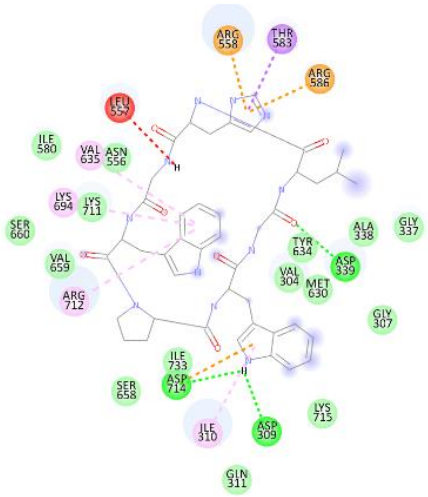	-10.9	Hydrogen Bonding with Asp714, Aso309, and Asp339; π-Cation or π-Anion interactions with Arg558, Asp714 and Arg586; π-Alkyl interactions with Ile310, Arg712, Lys694, and Val635.
2	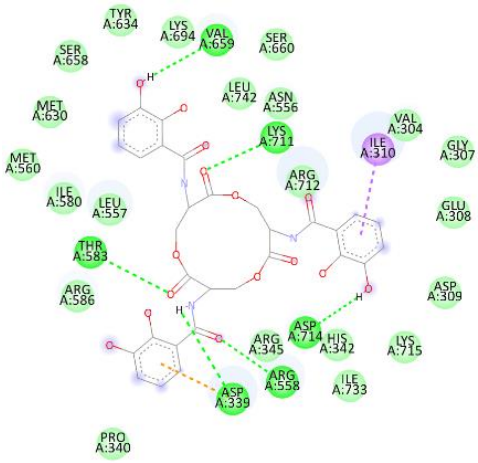	-10.9	Hydrogen Bonding with Val659, Thr583, Asp339, Arg558, and Asp714; π-Sigma interactions with Ile310.

1	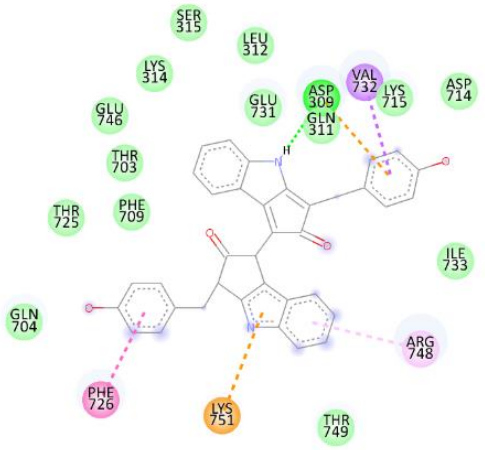	-10.4	Hydrogen Bonding with Asp309; π-Cation or π-Anion interaction with Lys751; π-Sigma interactions with Val732; π-Stacked interactions with Phe726; and π-Alkyl interactions Arg748.
			

Pharmacokinetics and Toxicity Predictions

Drug-likeness, pharmacokinetic properties, and toxicity predictions of the top-binding compounds **1**-**7** for each target protein were evaluated *in silico* using SwissADME and OSIRIS Property Explorer. The drug-likeness of each compound was evaluated based on Lipinski's Rule of Five, which focuses on the factors of molecular weight, a number of hydrogen acceptors and donors, and lipophilicity (Lipinski et al., 2012). The rule of five follows a set of range for each parameter, and a compound exhibits poor oral bioavailability when: molecular weight of a compound is less than or equal to 500 Da, lipophilicity is less than or equal to 5, hydrogen-bond donors are less than or equal to 5, and hydrogen-bond acceptors are less than or equal to 10. For the compounds to be druggable, violation is only limited to one (Daina et al., 2017; Lipinski et al., 2012). Based on these criteria, scytonemin (**1**), cryptophycin (**5**), and tjipanazole A2 (**6**) exhibited good oral bioavailability (Table 7). Among the three compounds that exhibited drug-likeness, compound **6** showed a high GI absorption. A BOILED-egg model was utilized to determine lipophilicity and polarity through WLOGP (atomistic octanol-water partition coefficient) and TPSA (topological polar surface area). The BOILED-egg model comprises of the yellow region or yolk, which determines that if the compound is inside the region, it has a high possibility of BBB permeation, as well as the white region of the model for passive absorption through the GI tract (Quimque et al., 2020). Compound **6** is located within the white region which means it has a high probability of GI absorption (Figure 3). In addition, *in silico* toxicity prediction in OSIRIS Property Explorer showed that compounds **2**-**4** and **6**-**7** were predicted to have no toxicity risks (Table 8). Compound **1** showed a high risk for reproductive toxicity and compound **5** also showed a high risk for mutagenicity. Among the seven compounds, based on the solubility predictions, compound **7** showed one of the best *S* log values of -3.62, and compound **2** showed the best solubility with an *S* log value of -2.41.

Table 7. Lipinski's "rule of five" for ADME analysis of compounds and drug-likeliness

Compound	Lipinski's rule of 5			
	Properties	Value	Violations	Lipinski
1	Molecular Weight (≤ 500Da)	544.55 Da	1	Yes
	LogP (≤ 5)	3.35		
	H-bond donor (≤ 5)	2		
	H-acceptor (≤ 10)	6		
	Rotatable Bonds (≤ 5)	3		
2	Molecular Weight (≤ 500Da)	669.55 Da	3	No
	LogP (≤ 5)	-1.77		
	H-bond donor (≤ 5)	9		
	H-acceptor (≤ 10)	15		
	Rotatable Bonds (≤ 5)	9		
3	Molecular Weight (≤ 500Da)	833.93 Da	3	No
	LogP (≤ 5)	-1.77		
	H-bond donor (≤ 5)	9		
	H-acceptor (≤ 10)	8		
	Rotatable Bonds (≤ 5)	8		
4	Molecular Weight (≤ 500Da)	1036.23 Da	3	No
	LogP (≤ 5)	-0.25		
	H-bond donor (≤ 5)	9		
	H-acceptor (≤ 10)	8		
	Rotatable Bonds (≤ 5)	9		
5	Molecular Weight (≤ 500Da)	655.18 Da	1	Yes
	LogP (≤ 5)	2.73		
	H-bond donor (≤ 5)	2		
	H-acceptor (≤ 10)	8		
	Rotatable Bonds (≤ 5)	8		
6	Molecular Weight (≤ 500Da)	471.33 Da	0	Yes
	LogP (≤ 5)	2.94		
	H-bond donor (≤ 5)	4		
	H-acceptor (≤ 10)	4		
	Rotatable Bonds (≤ 5)	1		
7	Molecular Weight (≤ 500Da)	705.71 Da	3	No
	LogP (≤ 5)	-0.13		
	H-bond donor (≤ 5)	8		
	H-acceptor (≤ 10)	13		
	Rotatable Bonds (≤ 5)	16		

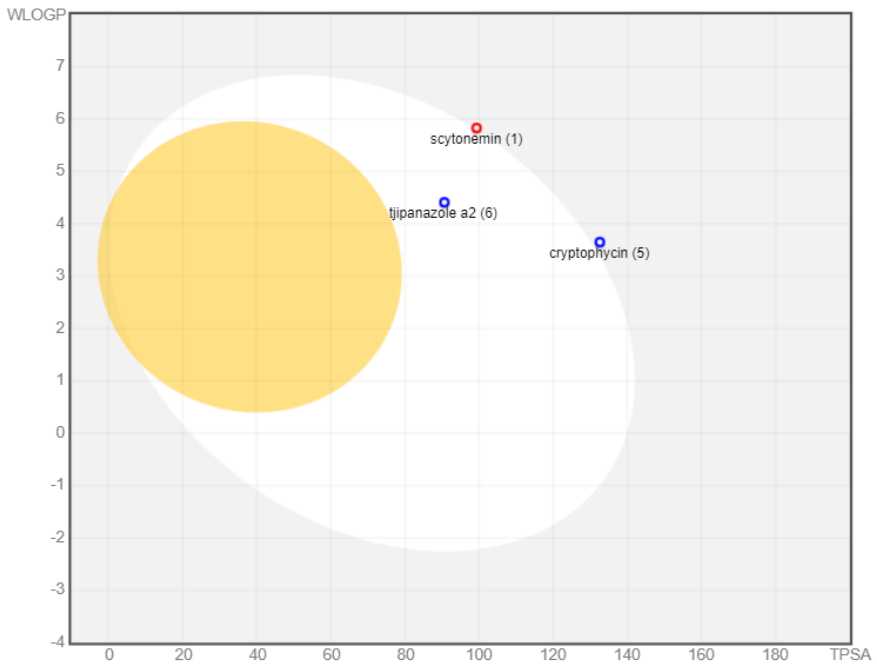

Figure 3. BOILED-egg plot of top cyanobacterial metabolites **1**, **5** and **6** for gastrointestinal tract absorption and BBB permeation.

Table 8. Toxicity and solubility predictions of compounds **1-7**.

Toxicity	**Compounds**						
	1	2	3	4	5	6	7
Mutagenicity	None	None	None	None	High Risk	None	None
Tumorgenicity	None	None	None	None	None	None	None
Irritant Effect	None	None	None	None	None	None	None
Reproductive	High Risk	None	None	None	None	None	None
Solubility (logS)	-5.55	-2.41	-4.81	-4.81	-5.97	-7.57	-3.62

With these, compound **1** is the best drug lead for SARS-CoV-2 since it passed the criteria for Lipinski's "rule of five" and showed an *in silico* antagonism against the five target proteins. It should also be noted that compound **6** showed the best pharmacokinetic property and drug-likeness among the top seven compounds. Despite having an *S* log value of -7.57, compound **6** showed absolutely no toxicity risks and was predicted with high GI absorption. Thus, compound **6** could also be a drug lead candidate against SARS-CoV-2.

DISCUSSION

Five proteins of SARS-CoV-2 in this study were selected and are known to portray important roles in host cell entry and viral replication. Like the host cell entry for SARS-CoV, SARS-CoV-2 binds to ACE2. Spike RBD ACE2 functions in host cell entry by binding to human ACE2. The comprehensive use of the SARS-CoV-2 spike indicates that it may have a wide host range, which explains the profound efficacy of ACE2 usage for host cell entry (Hu et al., 2020). It is also noted that the interactions of spike protein with host susceptibility factors, which includes receptors and proteases, were to infect human cells that contain hACE2 transmembrane proteins (Mittal et al., 2020). By entry through binding to epithelial cells in the respiratory tract, replication of SARS-CoV-2 is permitted for further infection (Hu et al., 2020). Aside from the active replication and release of the virus from lung cells, ACE2 receptors are distributed in different tissues in the body; thus, different symptoms are presented by the host (Cevik et al., 2020). Studies showed that host protease participates in cleaving the spike protein for the activation of cell entry of SARS-CoV-2 leading to its infection, which presents mild to severe symptoms, including respiratory failure. It also showed that antibodies with the help of convalescent plasma target the spike RBD ACE2 for them to be neutralized (Hu et al., 2020). Drug like umifenovir was found to be a potential treatment for COVID-19 since it targets the interaction between spike protein and ACE2 (Hu et al., 2020). Studies also showed that aside from ACE2 for host cell entry, glucose-regulated protein 78 (GRP78) can serve as an alternative receptor for SARS-CoV-2. It can translocate from the endoplasmic reticulum to the cell surface and acts like a coreceptor that signals molecules for viral entry (Carlos et al., 2021). On the other hand, non-structural proteins are highly conserved in Coronaviruses and have a significant role in post-translational modifications and viral replication (Li & Kang, 2020). Thus, with their functions, it is important to note them as drug targets against SARS-CoV-2 (de Leon et al., 2021). Among these nsps are the viral proteases that cleave the viral polyprotein to release other nsps. $3CL^{PRO}$ or non-structural protein 5 cleaves at 11 sites of the viral polyprotein to permit the replication of coronaviruses through the release of the functional

replicase complex and enable viral spread (Naidoo et al., 2020; Shin et al., 2020). RdRp or non-structural protein 12 plays an important role in the life cycle of SARS-CoV-2 as it is a core component of the viral replicase complex (Aftab *et al*., 2020). Remdesivir, which is widely used as a treatment for COVID-19, targets RdRp and can inhibit the synthesis of viral RNA (Jiang et al., 2020). In addition, PL^{PRO} or non-structural protein 3 is also an essential coronavirus enzyme that is required for cleavage at three sites of the viral polyprotein to produce a variety of non-structural proteins important for host modulation, combined with its deisolating and deubiquitylating activities (Shin et al., 2020; Tahir ul Qamar et al., 2020). In this study, several cyanobacterial metabolites were found to have high binding energies and showed multi-targeting activities to these target proteins. Scytonemin (**1**), was found to have a high binding affinity for all five target sites and proteins. Compound **1** was previously reported to have antimicrobial and anti-inflammatory activities (Swain et al., 2017; Vasas et al., 2010). Agardhipeptin A (**3**) exhibited high binding affinities for spike ACE2 RBD and PL^{PRO} as well as the highest binding energy for spike GRP78 RBD. Compound **3** was previously reported to have an enzyme inhibitor activity to serine and cysteine proteases (Rastogi & Sinha, 2009; Shin et al., 1996; Singh et al., 2017; Zainuddin et al., 2007). Cryptophycin (**5**) demonstrated a high binding affinity to RdRp. Compound **5** was recorded to have inhibitory properties against platinum-resistant ovarian cancer and advanced lung cancer (Swain et al., 2017). Vibriobactin (**7**), was found to have a favorable binding energy for $3CL^{PRO}$. Compound **7** was found to have a biological activity of a siderophore (Gademann & Portmann, 2008). Enterobactin (**2**) was found to have a high binding affinity for PL^{PRO}. Compound **2** was also previously reported to have a biological activity of a siderophore (Gademann & Portmann, 2008; Nowruzi et al., 2018) (Figure 4). The top seven compounds which showed an *in silico* antagonism to SARS-CoV-2, are first reported in this study to have potential antiviral properties.

These metabolites were further tested for drug-likeness, pharmacokinetic properties, and toxicity *in silico*. Lipinski's "rule of five" criteria was the basis in this study for the drug-likeness of

each compound. Implementation of this criteria sets the parameters for physiochemical properties to predict whether the compound has good oral absorption and permeation (Lipinski et al., 2012). In our study, a cyclic peptide, scytonemin (**1**) isolated from *Scytonema* sp. (Nowruzi et al., 2018; Rastogi & Sinha, 2009); a cytotoxin, cryptophycin (**5**) isolated from a lipophilic extract of *Nostoc* sp. ATCC 53789 (Nowruzi et al., 2018; Rastogi & Sinha, 2009); and an indole alkaloid, tjipanazole A2 (**6**) isolated from *Tolypothrix tjipanasensis* (Gademann & Portmann, 2008) were determined to be possible drug leads against SARS-CoV-2 since they exhibited favorable drug-like properties, high binding affinities, and good *in silico* toxicity predictions. It is also notable to mention agardhipeptin A (**3**) a cyclic peptide that is isolated from *Oscillatora agardhii* (Shin, H. J., Matsuda, H., Murakami, M., & Yamaguchi, K. 1996) showed an *in silico* antagonism against spike RBDs that are responsible for host cell entry of SARS-CoV-2, despite not meeting the criteria for Lipinski's "rule of five." Thus, these compounds must be subjected to *in vitro* screening using the appropriate cell line model for SARS-CoV-2 infection to confirm the *in silico* results.

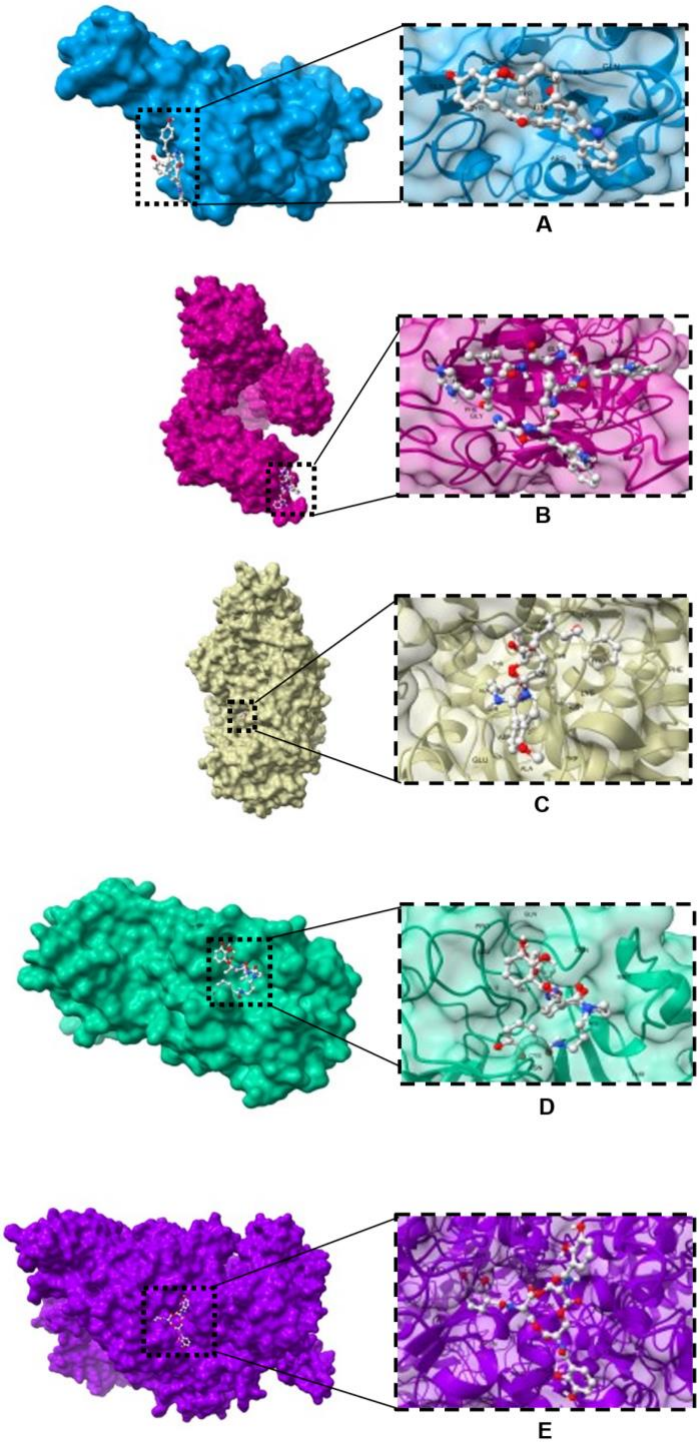

Figure 4. 3-Dimensional representation of the interaction of [A] scytonemin (**1**) in the binding site of Spike RBD ACE2; [B] agardhipeptin A (**3**) in the binding site of Spike RBD GRP78; [C] cryptophycin (**5**) in the binding site of RdRp; [D] vibriobactin (**7**) in the binding site of $3CL^{PRO}$; and [E] enterobactin (**2**) in the binding site of PL^{PRO}.

CONCLUSION

Cyanobacterial metabolites may potentially inhibit SARS-CoV-2 host cell entry and viral replication based on the results of our computational experiments. Seven compounds **1**–**7** was identified as top *in silico* antagonistic metabolites by their binding affinities against SARS-CoV-2 spike RBD for ACE2 and GRP78; and the nsps, $3CL^{PRO}$, PL^{PRO}, and RdRp. The multi-targeting cyanobacterial metabolites cyclic peptide scytonemin (**1**), cytotoxin cryptophycin (**5**), and an indole alkaloid tjipanazole A2 (**6**) may be presented as prototypes in the design of anti-COVID-19 drugs based on their high binding affinities and favorable pharmacokinetic properties.

STATEMENT ON CONFLICT OF INTEREST

No potential conflict of interest was declared by the authors.

REFERENCES

Africa, J. G. G., Arturo, H. C. P., Bernardo, L. J. M., Kyle, J., Ching, A. R., Casandra, O., Cruz, E. De, Hernandez, J. B. E., Magsipoc, R. J. Y., Sales, C. T. C., Agbay, J. C. M., Neri, G. L. L., Quimque, M. T. J., & Macabeo, A. P. G. (2022). In silico triple targeting of SARS-CoV-2 3CLpro, PLpro , and RdRp by Philippine antitubercular natural products libraries. Philippine Journal of Science, 151(1), 35–58.

Aftab, S. O., Ghouri, M. Z., Masood, M. U., Haider, Z., Khan, Z., Ahmad, A., & Munawar, N. (2020). Analysis of SARS-CoV-2 RNA-dependent RNA polymerase as a potential therapeutic drug target using a computational approach. Journal of Translational Medicine, 18(1), 1–15. https://doi.org/10.1186/s12967-020-02439-0

Albano, P. M., Notarte, K. I., Macaranas, I., & Maralit, B. (2020). Cross-contamination in Molecular Diagnostic Laboratories in Low- and Middle-income Countries: A Challenge to COVID-19 Testing. Philippine Journal of Pathology, 5(2), 7–11. https://doi.org/10.21141/pjp.2020.09

Brogi, S., Quimque, M. T., Notarte, K. I., Africa, J. G., Hernandez, B., Tan, S. M., Calderone, V., & Macabeo, A. P. (2022). Virtual Combinatorial Library Screening of Quinadoline B Derivatives against SARS-CoV-2 RNA-Dependent RNA Polymerase. Computation, 10(1), 7.

Carlos, A. J., Ha, D. P., Yeh, D. W., Van Krieken, R., Tseng, C. C., Zhang, P., Gill, P., Machida, K., & Lee, A. S. (2021). The chaperone GRP78 is a host auxiliary factor for SARS-CoV- 2 and GRP78 depleting antibody blocks viral entry and infection. Journal of Biological Chemistry, 296(23), 100759. https://doi.org/10.1016/J.JBC.2021.100759

Cevik, M., Kuppalli, K., Kindrachuk, J., & Peiris, M. (2020). Virology, transmission, and pathogenesis of SARS-CoV-2. The BMJ, 371, 1–6. https://doi.org/10.1136/bmj.m3862

Chaudhary, K. K., & Mishra, N. (2016). A Review on Molecular Docking: Novel Tool for Drug

Discovery. JSM Chem, 4(3), 1029.

Daina, A., Michielin, O., & Zoete, V. (2017). SwissADME: A free web tool to evaluate pharmacokinetics, drug-likeness and medicinal chemistry friendliness of small molecules. *Scientific Reports*, *7*(October 2016), 1–13. https://doi.org/10.1038/srep42717

de Leon, V. N. O., Manzano, J. A. H., Pilapil, D. Y. H., Fernandez, R. A. T., Ching, J. K. A. R., Quimque, M. T. J., Agbay, J. C. M., Notarte, K. I. R., & Macabeo, A. P. G. (2021). Anti-HIV reverse transcriptase plant polyphenolic natural products with in silico inhibitory properties on seven non-structural proteins vital in SARS-CoV-2 pathogenesis. Journal of Genetic Engineering and Biotechnology, 19(1), 1-17. https://doi.org/10.1186/s43141-021-00206-2

Fernandez, R. A., Quimque, M. T., Notarte, K. I., Manzano, J. A., Pilapil, D. Y., de Leon, V. N., San Jose, J. J., Villalobos, O., Muralidharan, N. H., Gromiha, M. M., Brogi, S., & Macabeo, A. P. G. (2021). Myxobacterial depsipeptide chondramides interrupt SARS-CoV-2 entry by targeting its broad, cell tropic spike protein. Journal of Biomolecular Structure and Dynamics, 1-12. https://doi.org/10.1080/07391102.2021.1969281

Gademann, K., & Portmann, C. (2008). Secondary Metabolites from Cyanobacteria: Complex Structures and Powerful Bioactivities. Current Organic Chemistry, 12(4), 326–341. https://doi.org/10.2174/138527208783743750

Hu, B., Guo, H., Zhou, P., & Shi, Z. L. (2020). Characteristics of SARS-CoV-2 and COVID-19. Nature Reviews Microbiology, 19(3), 141-154. https://doi.org/10.1038/s41579-020-00459-7

Jiang, Y., Yin, W., & Xu, H. E. (2020). RNA-dependent RNA polymerase: Structure, mechanism, and drug discovery for COVID-19. Biochemical and Biophysical Research Communications, 538, 47-53. https://doi.org/10.1016/j.bbrc.2020.08.116

Khateeb, J., Li, Y., & Zhang, H. (2021). Emerging SARS-CoV-2 variants of concern and potential intervention approaches. Critical Care, 25(1), 1–8. https://doi.org/10.1186/s13054-021-03662-x

Li, Q., & Kang, C. B. (2020). Progress in developing inhibitors of sars-cov-2 3c-like protease. Microorganisms, 8(8), 1–18. https://doi.org/10.3390/microorganisms8081250

Lipinski, C. A., Lombardo, F., Dominy, B. W., & Feeney, P. J. (2012). Experimental and computational approaches to estimate solubility and permeability in drug discovery and development settings. Advanced Drug Delivery Reviews, 64(SUPPL.), 4–17. https://doi.org/10.1016/j.addr.2012.09.019

Mittal, A., Manjunath, K., Ranjan, R. K., Kaushik, S., Kumar, S., & Verma, V. (2020). COVID-19 pandemic: Insights into structure, function, and hACE2 receptor recognition by SARS-CoV-2. PLoS Pathogens, 16(8), e1008762. https://doi.org/10.1371/journal.ppat.1008762

Naidoo, D., Roy, A., Kar, P., Mutanda, T., & Anandraj, A. (2020). Cyanobacterial metabolites as promising drug leads against the Mpro and PLpro of SARS-CoV-2: an in silico analysis. Journal of Biomolecular Structure and Dynamics, 0(0), 1–13. https://doi.org/10.1080/07391102.2020.1794972

Nowruzi, B., Haghighat, S., Fahimi, H., & Mohammadi, E. (2018). Nostoc cyanobacteria species: a new and rich source of novel bioactive compounds with pharmaceutical potential. Journal of Pharmaceutical Health Services Research, 9(1), 5–12. https://doi.org/10.1111/jphs.12202

Quimque, M. T. J., Notarte, K. I. R., Fernandez, R. A. T., Mendoza, M. A. O., Liman, R. A. D.,

Lim, J. A. K., Pilapil, L. A. E., Ong, J. K. H., Pastrana, A. M., Khan, A., Wei, D. Q., & Macabeo, A. P. G. (2021). Virtual screening-driven drug discovery of SARS-CoV2 enzyme inhibitors targeting viral attachment, replication, post-translational modification and host immunity evasion infection mechanisms. Journal of Biomolecular Structure and Dynamics, 39(12), 4316–4333. https://doi.org/10.1080/07391102.2020.1776639

Quimque, M. T., Notarte, K. I., Adviento, X. A., Cabunoc, M. H., de Leon, V. N., Delos Reyes, F. S. L., Lugtu, E. J., Manzano, J. A., Monton, S. N., Muñoz, J. E., Ong, K. D., Pilapil Iv, D. Y., Roque Iii, V., Tan, S. M., Lim, J. A., & Macabeo, A. P. (2021). Polyphenolic Natural Products Active In Silico against SARS-CoV-2 Spike Receptor Binding Domains and Non-Structural Proteins - A Review. Combinatorial Chemistry & High Throughput Screening. https://doi.org/10.2174/1386207325666210917113207

Raja, R., Hemaiswarya, S., Ganesan, V., & Carvalho, I. S. (2016). Recent developments in therapeutic applications of Cyanobacteria. Critical Reviews in Microbiology, 42(3), 394–405. https://doi.org/10.3109/1040841X.2014.957640

Rastogi, R. P., & Sinha, R. P. (2009). Biotechnological and industrial significance of cyanobacterial secondary metabolites. Biotechnology Advances, 27(4), 521–539. https://doi.org/10.1016/j.biotechadv.2009.04.009

Shin, D., Mukherjee, R., Grewe, D., Bojkova, D., Baek, K., Bhattacharya, A., Schulz, L., Widera, M., Mehdipour, A. R., Tascher, G., Geurink, P. P., Wilhelm, A., van der Heden van Noort, G. J., Ovaa, H., Müller, S., Knobeloch, K. P., Rajalingam, K., Schulman, B. A., Cinatl, J., … Dikic, I. (2020). Papain-like protease regulates SARS-CoV-2 viral spread and innate immunity. Nature, 587(7835), 657–662. https://doi.org/10.1038/s41586-020-2601-5

Tahir ul Qamar, M., Alqahtani, S. M., Alamri, M. A., & Chen, L. L. (2020). Structural basis of SARS-CoV-2 3CLpro and anti-COVID-19 drug discovery from medicinal plants. Journal of Pharmaceutical Analysis, 10(4), 313–319. https://doi.org/10.1016/j.jpha.2020.03.009

van Dorp, L., Acman, M., Richard, D., Shaw, L. P., Ford, C. E., Ormond, L., Owen, C. J., Pang, J., Tan, C. C. S., Boshier, F. A. T., Ortiz, A. T., & Balloux, F. (2020). Emergence of genomic diversity and recurrent mutations in SARS-CoV-2. Infection, Genetics and Evolution, 83(April), 104351. https://doi.org/10.1016/j.meegid.2020.104351

Walls, A. C., Park, Y. J., Tortorici, M. A., Wall, A., McGuire, A. T., Veesler, D. 2020. Structure, Function, and Antigenicity of the SARS-CoV-2 Spike Glycoprotein. Cell, 181(2): 281-292. https://doi.org/10.1016/j.cell.2020.02.058